Scientia Iranica A (2021) 28(5), 2493–2503

Sharif University of Technology
Scientia Iranica
Transactions A: Civil Engineering
http://scientiairanica.sharif.edu

A solution for unconfined groundwater flow: An innovative approach based on the lattice Boltzmann method

R. Yousefi[a], N. Talebbeydokhti[a], S.H. Afzali[a], and A.A. Hekmatzadeh[b,*]

a. *Department of Civil and Environmental Engineering, School of Engineering, Shiraz University, Shiraz, Iran.*
b. *Department of Civil and Environmental Engineering, Shiraz University of Technology, Shiraz, P.O. Box 71555-313, Iran.*

Received 29 April 2020; received in revised form 27 November 2020; accepted 12 April 2021

KEYWORDS
Lattice Boltzmann Method (LBM); Groundwater flow; Numerical solution; Unconfined aquifer; D2Q9 scheme.

Abstract. Lattice Boltzmann Method (LBM) has emerged as a fast, precise, and efficient numerical solution to solve differential equations. There seems to be a lack of research on the use of LBM to solve groundwater flow in unconfined aquifers. Therefore, in this study, considering the D2Q9 scheme, an innovative numerical solution based on LBM was introduced to solve the groundwater flow in unconfined aquifers. The solutions obtained from the proposed LBM were compared to results that stemmed from three different unconfined groundwater problems with known solutions. Both steady and transient conditions for groundwater flow were considered in simulations. The results showed that the proposed LBM can satisfactorily simulate unconfined groundwater flow.

1. Introduction

The Lattice Boltzmann Method (LBM) is considered a robust numerical technique to solve time-dependent problems, benefiting from high accuracy, simulation of complicated boundary conditions, and simplicity in the computer code operation [1]. Moreover, the LBM benefit from the fast computational ability and admirable stability, especially in time-dependent problems. This method show superior capability to fulfill the requirements of parallel programing techniques using graphics processing units [2,3]

This method has various applications in the simulation of different physical phenomena such as solitary wave [4], convection-diffusion equations [5], shallow water [6], heat conduction [7], and kinetic equations [8]. In the last decade, this method has been employed to simulate mass transfer problems such as groundwater flow equation and solute transport equation. The diffusion equation governs groundwater flow, while the advection-diffusion equation describes the solute transport [2,9,10]. It is worth noting that various lattice configurations have been developed for LBM to solve mass transfer equations, containing D1Q2 and D1Q3 for one-dimensional problems, D2Q4, D2D5, and D2Q9 for two-dimensional problems, in addition to, D3Q15 and D3Q19 for the three dimensions [3,11–13].

Regarding the advection-diffusion equation, bulks of studies have been carried out to solve this equation using the above-mentioned lattice forms. Early studies were focused on the solution of the advection-diffusion equation with constant coefficients [12,14–16]. In recent years, the advection-diffusion equation with vari-

*. *Corresponding author. Tel./Fax: +98 71 37277656*
E-mail addresses: roghaieyousefi@yahoo.com (R. Yousefi); taleb@shirazu.ac.ir (N. Talebbeydokhti); afzali@shirazu.ac.ir (S.H. Afzali); hekmatzadeh@sutech.ac.ir (A.A. Hekmatzadeh)

doi: 10.24200/sci.2021.55624.4321

able constant in Cartesian or cylindrical coordinates has also been solved using LBM [17–20]. It is worth noting that in the numeral simulation using LBM [21–24], the applications of two or More Relaxation Times (MRT) instead of a single relaxation time are also considered. Regarding MRT-based schemes, Guo et al. indicated that the collision matrix in the MRT-based LBM for advection-dispersion equation guarantees the second-order accuracy of the half-way anti-bounce-back scheme [24]. Recently, taking into account the moving boundary conditions, Zhang and Misbah developed an LBM to solve the advection-dispersion equation [25]. Moreover, Du and Liu employed double-distribution functions to solve fractional advection-diffusion problem combined with incompressible Navier-Stokes equations [26].

Considering diffusion equation as groundwater flow, Wolf-Gladrow [27] used LBM to solve the diffusion equation for the first time. Lin et al. [28] used LBM to describe reaction-diffusion of five chemical components in a porous catalyst with a macro-mesopore structure. In the context of groundwater flow, Zhou solved the groundwater equation using LBM in both one and two dimensions [29]. The results showed that LBM has high accuracy in simulating groundwater flow in a confined aquifer. Furthermore, Zhou improved the application of LBM in the rectangular lattice configuration to simulate the groundwater flow [30]. Anwar and Sukop [31] simulated solute transport and transient groundwater flow using both diffusion-based LBM and Navier-Stokes-based LBM. In doing so, they employed the altered-velocity model in the simulations with the latter method. Moreover, the lattice Boltzmann solution for groundwater flow in non-orthogonal structured lattices was developed by Budinski et al. [32].

In addition, the joint solutions of groundwater flow and pollutant transport using LBM have so far been performed in several studies [33,34]. The combination of LBM and other numerical schemes has also been used to solve mass transportation problems. For instance, a lattice Boltzmann solution was developed by Liu et al. to solve the radiative transfer problems in both steady and transient states. They employed a forward difference scheme for the time derivative of the source term in the evolution equation, which guarantees stability and accuracy [35]. Yu et al. developed a coupled lattice Boltzmann/finite difference method to simulate the dynamics of fluid flow, advection, diffusion, and adsorption in porous media. In this approach, the single-relaxation time LBM is hired for the fluid dynamics, while the advection-diffusion equation is solved by using the finite difference method [10].

To the best of our knowledge, the existing lattice Boltzmann solutions for groundwater flow are mainly associated with a confined aquifer, where the state variable is head. The general form of groundwater equation in three dimensions is written as Eq. (1) [36]:

$$\frac{\partial h}{\partial t} = \frac{T}{S}\nabla^2 h + \frac{R}{S}, \tag{1}$$

where h is the groundwater head, T and S represent transmissivity and storativity, respectively, and R is the recharge function. This equation describes transient groundwater flow in both confined and unconfined aquifers. However, for the case of an unconfined aquifer, the new location of the water table at every time step should be considered in the mesh generation. In other words, adaptive mesh refinement should be included in the simulations. Assuming the flow happens through the entire vertical cross-section, Eq. (1) may be converted to a two-dimensional equation as follows:

$$\frac{\partial h}{\partial t} = \frac{K}{S_y}\left(\frac{\partial^2 (h^2/2)}{\partial x^2} + \frac{\partial^2 (h^2/2)}{\partial y^2}\right) + \frac{R}{S_y}, \tag{2}$$

where K is the hydraulic conductivity and S_y represents the specific yield. It is worthy to note that S_y is a dimensionless quantity, ranging between 0 and 0.4.

In terms of an unconfined aquifer wherein the state variable (i.e. h^2) is of second order, the solution of groundwater flow using lattice Boltzmann has not been described satisfactorily. Therefore, in this research, an innovative framework is introduced to solve the problem of groundwater flow in the unconfined aquifer (i.e. Eq. (2)). For solving differential equations using LBM, the form of the balanced distribution function plays a key role in the formulations. Here, a new local equilibrium distribution function related to the D2Q9 configuration is proposed to solve the problem of groundwater flow in unconfined aquifers. Accordingly, Eq. (2) is recovered from the Chapman-Enskog expansion using the new proposed equilibrium distribution function. To validate the new formulations, not only the steady problem in the unconfined aquifer but also the transient problem are considered. Also, sensitivity analysis of relaxation time is performed considering 8 different values.

2. Lattic Boltzmann Method (LBM)

The lattice Boltzmann equation (Eq. (3)) is applied to formulate groundwater flow in an unconfined aquifer [11]:

$$f_k(x + c_k\Delta t, t + \Delta t) = f_k(x,t) + \frac{1}{\tau}[f_k^{eq}(x,t) - f_k(x,t)] + \frac{R}{aS_y}\Delta t, \tag{3}$$

where f_k is the particle distribution function, f_k^{eq} represents the local equilibrium distribution function,

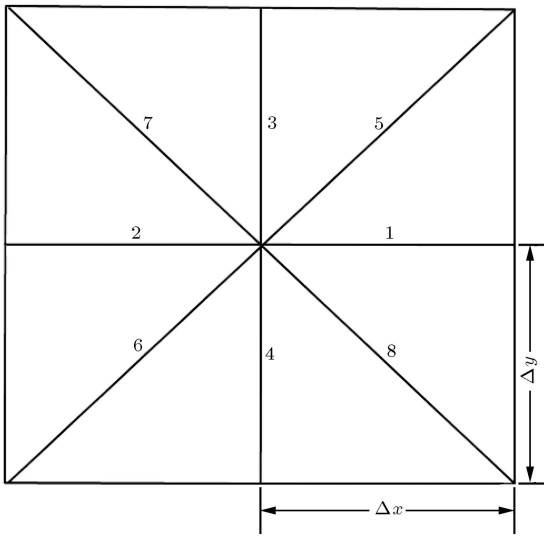

Figure 1. Nine-velocity rectangular lattice (D2Q9).

Δt is the time step, x is the space vector in x, y coordinate system, c_k is the particle velocity vector, τ indicates the single relaxation time, and a is the number of the particle velocity. Herein, the D2Q9 lattice configuration was employed for the numerical solution (Figure 1), consequently, $a = 9$. In addition, c_k, which represents the celerity $c_x = \Delta x/\Delta t$, is defined by Eq. (4) [37]:

$$\begin{aligned} c_k &= (0,0) && k = 0, \\ c_k &= (\pm c_x, 0), (0, \pm c_y) && k = 1,2,3,4, \\ c_k &= (\pm c_x, \pm c_y) && k = 5,6,7,8. \end{aligned} \tag{4}$$

In Eq. (3), f_k is defined by Eq. (5):

$$f_k(x,t) = w_k h(x,t), \tag{5}$$

where $h(x,t)$ is the water head and w is a weight factor for every direction according to the following expressions:

$$\begin{aligned} w_0 &= \frac{4}{9}, \\ w_1 = w_2 = w_3 = w_4 &= \frac{1}{9}, \\ w_5 = w_6 = w_7 = w_8 &= \frac{1}{36}. \end{aligned} \tag{6}$$

2.1. Boundary conditions

In the problems considered in this study, four types of boundary conditions are considered in the simulation of groundwater flow, including the Dirichlet and Neumann boundary conditions, in addition to the open and solid boundary conditions in line with Eq. (7) to Eq. (10) [38]. It should be pointed out that the boundary conditions for each groundwater flow problem are described in Section 5.

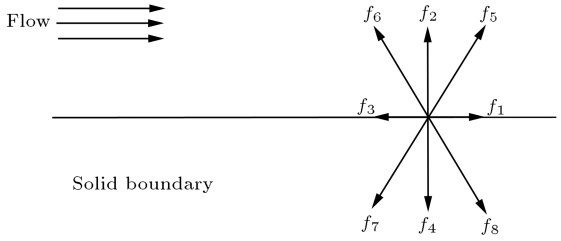

Figure 2. Solid boundary condition.

Considering Figure 2, the distribution functions at solid boundary (southern boundary) is estimated using Eq. (7):

$$f_2 = f_4, \qquad f_5 = f_7, \qquad f_6 = f_8. \tag{7}$$

If the open boundary is assumed for the easternboundary in Figure 2, then Eq. (8) is used to compute distribution functions:

$$\begin{aligned} f_3(i=m,j) &= 2 \times f_3(i=m-1,j) - f_3(i=m-2,j), \\ f_6(i=m,j) &= 2 \times f_6(i=m-1,j) - f_6(i=m-2,j), \\ f_7(i=m,j) &= 2 \times f_7(i=m-1,j) - f_7(i=m-2,j). \end{aligned} \tag{8}$$

In terms of Dirichlet boundary condition at the western boundary in Figure 2, Eq. (9) is applied so as to calculate the distribution functions:

$$\begin{aligned} f_1 &= (w_1 + w_3) \times h - f_3, \\ f_5 &= (w_5 + w_7) \times h - f_7, \\ f_8 &= (w_8 + w_6) \times h - f_6. \end{aligned} \tag{9}$$

The distribution function in the case of Neumann boundary condition (northern boundary in Figure 2) is determined from Eq. (10):

$$\begin{aligned} f_4(i.j = n) &= f_4(i.j = n-1), \\ f_7(i.j = n) &= f_7(i.j = n-1), \\ f_8(i.j = n) &= f_8(i.j = n-1). \end{aligned} \tag{10}$$

3. Derivation of unconfined groundwater equation from LBM

Zhou [1] introduced a new local equilibrium distribution function to solve the convection-dispersion equation. Inspiring from the above-mentioned methodology, the following equation was innovatively defined in this

study for the equilibrium distribution function (f_k^{eq}) as follows:

$$f_k^{eq}=h-\frac{K}{S_y}\left(\frac{1}{\Delta t c^2(\tau-0.5)}\right)\frac{h^2}{2} \qquad k=0,$$

$$f_k^{eq}=\frac{1}{4}\frac{K}{S_y}\left(\frac{1}{\Delta t c^2(\tau-0.5)}\right)\frac{h^2}{2} \qquad k=1,2,3,4,$$

$$f_k^{eq}=-\frac{K}{S_y}\left(\frac{1}{4\Delta t c_{kx}c_{ky}(\tau-0.5)}\right)\frac{h^2}{2} \qquad k=5,6,7,8. \tag{11}$$

Eq. (11) satisfies three properties, including mass balances, momentum, and energy conservation according to Eqs. (12)–(14):

$$\sum_k f_k^{eq}(x,t)=h(x,t), \tag{12}$$

$$\sum_k c_{ki}f_k^{eq}(x,t)=0, \tag{13}$$

$$\sum_k c_{ki}c_{kj}f_k^{eq}(x,t)=\frac{\left(\frac{K}{S_y}\right)_{ij}}{\Delta t(\tau-0.5)}\frac{h^2(x,t)}{2}. \tag{14}$$

Taking into account the proposed equilibrium distribution function (Eq. (11)) and their properties (Eqs. (12)–(14)), groundwater head is obtained using Eq. (15):

$$h=\sum_k f_k(x,t). \tag{15}$$

To correlate the head obtained in Eq. (15) with the groundwater flow equation in the unconfined aquifer (Eq. (2)), the Chapman-Enskog expansion is used. Assuming small $t(\Delta t=\varepsilon)$ and substituting ε instead of Δt, Eq. (3) is converted to Eq. (16):

$$f_k(x+c_k\varepsilon,t+\varepsilon)=f_k(x,t)+\frac{1}{\tau}[f_k^{eq}(x,t)-f_k(x,t)]+\frac{R}{aS_y}\varepsilon. \tag{16}$$

In line with the Chapman-Enskog expansion, f is described by Eq. (17) [11]:

$$f_k=f_k^0+\varepsilon f_k^{(1)}+\varepsilon^2 f_k^{(2)}. \tag{17}$$

Employing the centered scheme suggested by Zhou, the recharge function is expressed by Eq. (18) [37]:

$$\frac{R}{aS_y}=\frac{R}{aS_y}\left(x+\frac{1}{2}c_k\varepsilon,t+\frac{1}{2}t\right). \tag{18}$$

Considering Taylor expansion, Eqs. (19) and (20) are derived from Eqs. (16) and (18) stated as:

$$\varepsilon\left(\frac{\partial}{\partial t}+c_{ki}\frac{\partial}{\partial x_i}\right)f_k+\frac{1}{2}\varepsilon^2\left(\frac{\partial}{\partial t}+c_{ki}\frac{\partial}{\partial x_i}\right)^2 f_k=\frac{R}{aS_y}\varepsilon-\frac{1}{\tau}(f_k-f_k^{eq}), \tag{19}$$

$$\frac{R}{aS_y}\left(x+\frac{1}{2}c_k\varepsilon,t+\frac{1}{2}t\right)=\frac{R}{aS_y}(x,t)+\frac{1}{2}\varepsilon\left(\frac{\partial}{\partial t}+c_{ki}\frac{\partial}{\partial x_i}\right)\frac{R}{aS_y}. \tag{20}$$

If Eqs. (17) and (20) are inserted in Eq. (19), the following relations are achieved for the coefficients of ε^0, ε^1, and ε^2:

coefficients of ε^0:

$$f_k^{(0)}=f_k^{eq}, \tag{21}$$

coefficients of ε^1:

$$\left(\frac{\partial}{\partial t}+c_{ki}\frac{\partial}{\partial x_i}\right)f_k^{(0)}=-\frac{1}{\tau}f_k^{(1)}+\frac{R}{aS_y}, \tag{22}$$

coefficients of ε^2:

$$\left(\frac{\partial}{\partial t}+c_{ki}\frac{\partial}{\partial x_i}\right)f_k^{(1)}+\frac{1}{2}\left(\frac{\partial}{\partial t}+c_{ki}\frac{\partial}{\partial x_i}\right)^2 f_k^{(0)}=-\frac{1}{\tau}f_k^{(2)}+\frac{1}{2}\left(\frac{\partial}{\partial t}+c_{ki}\frac{\partial}{\partial x_i}\right)\frac{R}{aS_y}. \tag{23}$$

The placement of Eq. (22) into Eq. (23) leads to Eq. (24):

$$\left(\frac{1}{2\tau}-1\right)\left(\frac{\partial}{\partial t}+c_{ki}\frac{\partial}{\partial x_i}\right)f_k^{(1)}=\frac{1}{\tau}f_k^{(2)}. \tag{24}$$

Afterward, Eq. (25) is derived by considering $\varepsilon\times$ Eq. (24) and adding it to Eq. (22):

$$\left(\frac{\partial}{\partial t}+c_{ki}\frac{\partial}{\partial x_i}\right)f_k^{(0)}+\varepsilon\left(1-\frac{1}{2\tau}\right)\left(\frac{\partial}{\partial t}+c_{ki}\frac{\partial}{\partial x_i}\right)f_k^{(1)}=-\frac{1}{\tau}(f_k^{(1)}-\varepsilon f_k^{(2)})+\frac{R}{aS_y}, \tag{25}$$

and Eq. (26) is obtained by substituting Eq. (21) into Eq. (25) and then applying the summation ($\sum$):

$$\frac{\partial}{\partial t}\sum_k f_k^{eq}+\frac{\partial}{\partial x_i}\sum_k c_{ki}f_k^{eq}=\varepsilon\left(\tau-\frac{1}{2}\right)\frac{\partial}{\partial x_i}\sum_k c_{ki}c_{kj}\frac{\partial f_k^{(0)}}{\partial x_i}+\frac{R}{S_y}+\varepsilon\left(\tau-\frac{1}{2}\right)\frac{\partial}{\partial x_i}\frac{\partial}{\partial t}\sum_k c_{ki}f_k^{(0)}. \tag{26}$$

Table 1. Coordinates of pumping wells and the values of their pumping rates [29].

Number	1	2	3	4	5	6	7	8	9	10
X (m)	1250	2250	3250	1250	2250	3250	1250	2000	2500	3250
Y (m)	8500	8500	8500	5000	5000	5000	3500	3500	3500	3500
Q (m^3/day)	7000	7000	7000	5960	4503	5949	6729	4282	4230	6807

The above equation is transformed to Eq. (27) by replacing ε with Δt, taking into account the properties of f^{eq}:

$$\frac{\partial h}{\partial t}=\frac{K}{S_y}\frac{\partial^2(h^2/2)}{\partial x_i^2}+\frac{R}{S_y}+\varepsilon\left(\tau-\frac{1}{2}\right)\frac{\partial}{\partial x_i}\frac{\partial}{\partial t}\sum_k c_{ki}f_k^{(0)}. \tag{27}$$

According to the properties of f^{eq}, the last term on the right-hand side of Eq. (26) is also zero, thus the groundwater flow equation in the unconfined aquifer (Eq. (2)) is derived.

4. Validation of the proposed LBM

Three unconfined groundwater problems with known solutions were considered to validate the accuracy and capability of the proposed LBM to solve the groundwater flow in an unconfined aquifer. The solutions of two real problems were documented in U.S. geological survey modular finite difference flow model (MODFLOW), whereas an analytical solution was found in the study of El-Ghandour and Elsaid [39].

4.1. Problem 1

A groundwater problem, solved analytically by El-Ghandour and Elsaid in 2013 [39], was considered for the validation of the proposed LBM (Figure 3). In this problem, water was extracted from 10 pumping wells in an unconfined aquifer with a length of 10000 m, a width of 4500 m, and a thickness of 100 m. The hydraulic conductivity and the specific yield are 50 m/day and 0.1, respectively. A constant head of 20 m was considered for both northern and southern boundaries, whereas a solid boundary condition (no flow boundary) was assumed for the left and right borders. The location and pumping rates of the mentioned wells are reported in Table 1. In addition, a recharge rate of 0.001 m/day was assumed.

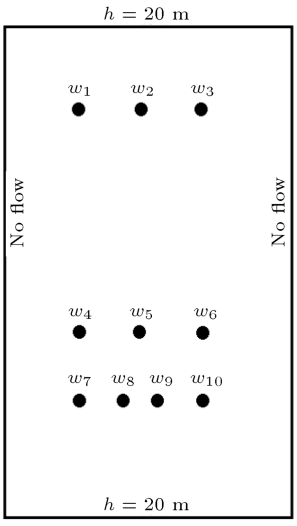

Figure 3. Plan view of aquifer (Problem 1) [39].

4.1.1. Results of problem 1

The steady-state solution was considered in this problem. The head contour lines stemmed from LBM, and analytical solutions are depicted in Figure 4. Accordingly, high levels of agreement are qualitatively observed between the analytical and numerical head values. In addition, the small Relative Errors (REs) confirm the high consistency between the analytical solution results and the lattice Boltzmann results . The REs between the estimations from LBM and analytical solution (Eq. (28)) at the location of wells (see Figure 4) are given in Table 2, indicating an average value of 0.0053. The grid size along the x and y direction was chosen to be 50 m (200 × 90 square lattices). In the above computations, the relaxation time was

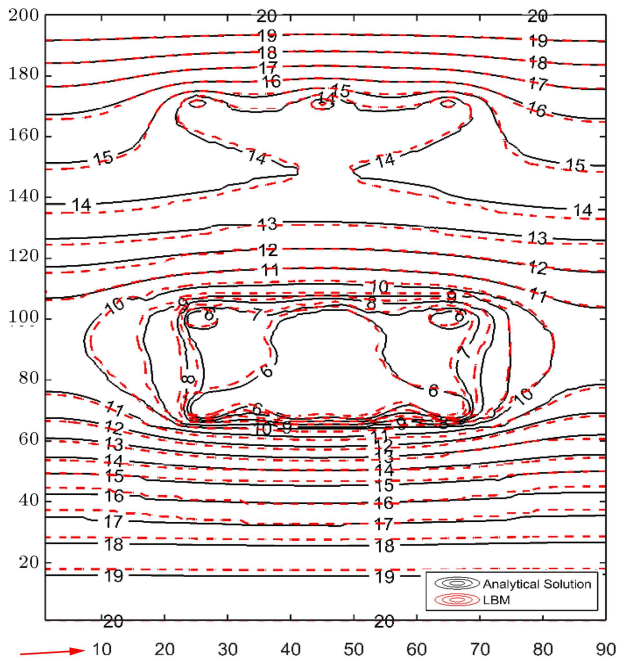

Figure 4. Head contour obtained from analytical solution and Lattic Boltzmann Method (LBM) (Problem 1).

Table 2. Relative Errors (REs) at the location of wells (Problem 1) with the grid size of 50 m.

Wells	$w1$	$w2$	$w3$	$w4$	$w5$	$w6$	$w7$	$w8$	$w9$	$w10$
RE	0.005	0.007	0.004	0.005	0.004	0.006	0.007	0.005	0.004	0.006

Table 3. Relative Errors (REs) at the location of wells (Problem 1) with the grid size of 25 m.

Wells	$w1$	$w2$	$w3$	$w4$	$w5$	$w6$	$w7$	$w8$	$w9$	$w10$
RE	0.004	0.005	0.004	0.004	0.004	0.005	0.005	0.004	0.004	0.004

considered to be 0.75, and a time step of 0.002 day (considering stability criteria) was selected.

$$RE = \frac{\text{LBM} - \text{analytical solution}}{\text{analytical solution}}. \quad (28)$$

It is worth noting that the groundwater flow solution in which the numerical methods are used is not as accurate as of the related analytical solution. In addition, the computational time of analytical solutions is usually lower than that of the numerical methods. However, the analytical solution is not available for every geometry and boundary condition. In this example, it was observed that the presented LBM has satisfactory accuracy compared to the analytical solution.

4.1.2. The effect of grid size

To examine the effect of the mesh size on the aforementioned problem, the 25 m grid size along the x and y directions was also considered. The relative errors (REs) between the results of the LB method and the analytical solutions for each well location are shown in Table 3. Accordingly, the REs are nearly 0.001 smaller than the errors reported in Table 2, indicating that by halving the grid dimension, the increase in accuracy could be considered negligible.

4.1.3. Sensitivity analysis regarding relaxation time

In order to check the effects of relaxation time on the numerical solution, sensitivity analysis was performed. Figure 5 shows the estimated relative errors at every well for different τ values. The relaxation times varied between 0.72 and 0.85. Accordingly, the RE values are small when the relation time is between 0.72 and 0.77. However, the REs increase once the relaxation becomes greater than 0.8. It should be noted that the above-mentioned sensitivity analysis is associated with Problem 1 since the value of relaxation time depends on the problem conditions and mesh resolution [1].

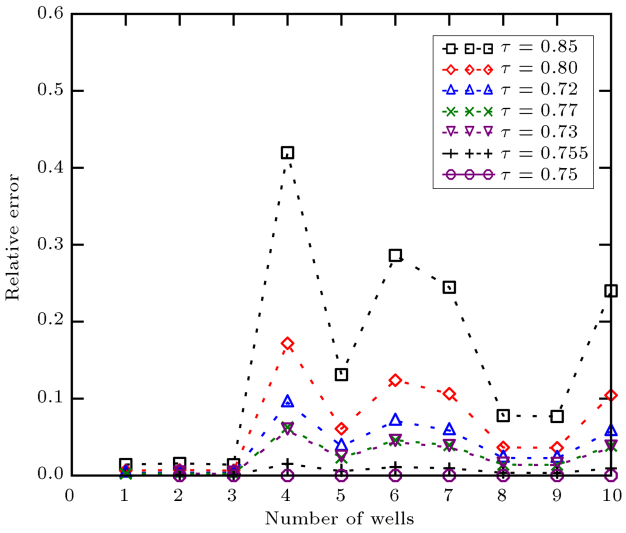

Figure 5. Relative errors between the water head considering $\tau = 0.75$ and the other values of τ at the location of wells (Problem 1).

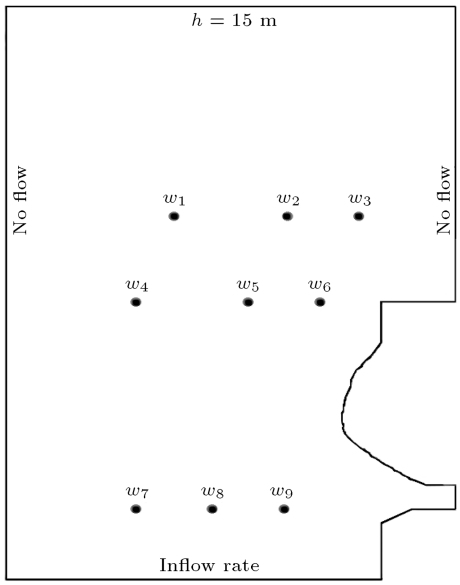

Figure 6. Plan view of aquifer (Problem 2) [46].

4.2. Problems 2

There are several instances of unconfined groundwater flow examples with analytical solutions in the literature [40–45]. However, these solutions are mainly associated with regular borders. To assess the ability of the proposed LB procedure in irregular borders, an unconfined groundwater example shown in Figure 6 was considered. The hydraulic conductivity of 160 m/day and specific yield of 0.06 was assumed in this problem. Along the eastern and western sides of the aquifer, the boundaries were set as solid boundaries. In the southeastern corner, a mountain (curve boundary) is

presumed. In the northern border, a constant hydraulic head of 15 m (Dirichlet condition) was assumed, while a specified flux rate of 0.0672 m^3/day per meter (Neumann condition) was considered on the southern edge. The aquifer was 10000 m long, 6000 m wide, and 25 m deep, containing 9 pumping wells. Depending on the pumping rate on the plain, both steady and transient conditions were considered [46].

In the steady-state problem (first step), the pumping rates were zero, whereas the recharge rate on the plain was 0.00025 m/day. The initial head in the borders was 16 m. The results of steady-state simulation were used as the initial starting heads for the transient state. When the pumping wells start water extraction from the aquifer, the problem becomes transient (second step). Therein, the pumping rates were equal to 3888 m^3/day during the 8-month of dry seasons. In the third step, it is assumed that there is no pumping for the 4-month wet season after the 8-month dry season. Herein, the recharge rate is set to 0.00075 m/day. It should be noted that the results obtained at the termination time of the prior step consider the initial conditions for the transient problem in the third step.

4.2.1. Results of Problem 2

This problem was simulated in three steps of steady and transient states in three steps. The head contours of all steady and transient steps, arisen from both LBM and MODFLOW simulations, are depicted in Figure 6. Accordingly, a high level of match is perceived between the head contours, indicating the capability of the introduced LBM for modeling this problem. In addition, the values of REs between the heads resulted from both methods (LBM and MODFLOW) were compared in the observation wells, as shown in Figure 7. In line with Table 4, the small values of REs confirm appreciable agreements between the estimations of MODFLOW and LBM. The average values of RE for the first, second, and third steps were 0.003, 0.006, and 0.003, respectively. The results demonstrate the proposed LBM has a good ability to model the unconfined aquifer with curve boundaries. In this problem, the mesh size for the first and third steps was set to $\Delta x = \Delta y =$ 500 m. For the second step, a square mesh of 167 m was considered. Considering the stability criterion, the values of τ and Δt were equal to 0.75 and 0.001 day, respectively.

Table 5. Relative errors (REs) at P1-P5 locations (Problem 3).

Points		$P1$	$P2$	$P3$	$P4$	$P5$
Location	Row	25	25	25	25	25
	Column	5	15	25	35	45
RE_step one		0.003	0.002	0.001	0.001	0.002
RE_step two		0.001	0.001	0.002	0.002	0.001

4.3. Problem 3

For the third case, an unconfined aquifer with the domain size of 1000 m long, 1000 m wide, and 120 m high was considered (Figure 8) [46]. A pumping well exists in this aquifer at $x = 800$ m and $y = 500$ m (Figure 8). The hydraulic conductivity of the aquifer is 0.5 m/day and the specific yield is 0.001. There is a constant head of 100 m and 80 m at the eastern and western boundaries, respectively. The southern and northern boundaries are considered solid boundaries. The problem is solved in two steps only under steady-state conditions. In the first step, a recharge rate of 0.00323 m/day is considered. The initial head is shown in Figure 8.

In the second step, the recharge rate and well pump flow rate were 0.00323 m/day and 2000 m^3/day, respectively. The head obtained in step one is used as the initial conditions for this step.

4.3.1. Results of Problem 3

Figure 9 depicts the head contours obtained from LBM and MODFLOW in both steps, indicating the close agreement between the solutions of LBM and those of MODFLOW. For these two steps, the RE between LBM and MODFLOW simulations at the points displayed in Figure 8 are given in Table 5. The average values of RE are 0.002 and 0.001 for steps one and two, respectively, confirming small differences between LBM and MODFLOW solutions. Herein, $\Delta x = \Delta y = 20$ m, $\tau = 0.7$, and $\Delta t = 0.01$ day. These results obtained from the above-mentioned problems indicated that the introduced LBM is an appropriate numerical method for the solution of the groundwater problems in unconfined aquifers.

5. Conclusions

In the present study, the groundwater flow in an unconfined aquifer was solved innovatively using Lattic Boltzmann Method (LBM). A new form of equilibrium

Table 4. Relative Error (REs) at the location of wells (Problem 2).

Wells	$w1$	$w2$	$w3$	$w4$	$w5$	$w6$	$w7$	$w8$	$w9$
RE_step one	0.004	0.003	0.002	0.002	0.003	0.003	0.002	0.003	0.003
RE_step two	0.005	0.005	0.004	0.006	0.005	0.006	0.004	0.007	0.008
RE_step three	0.003	0.004	0.002	0.003	0.002	0.004	0.002	0.003	0.002

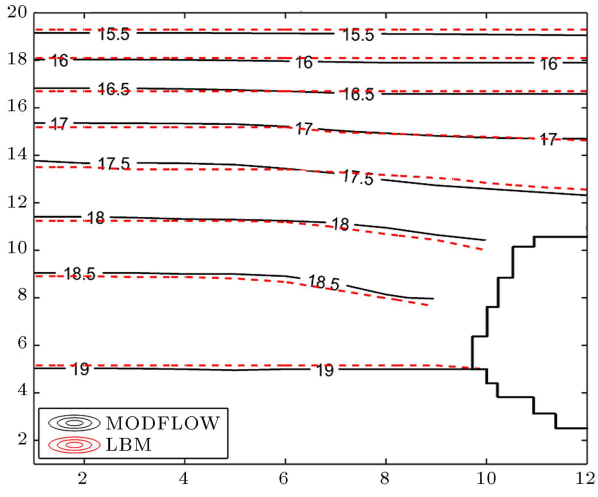

(a)

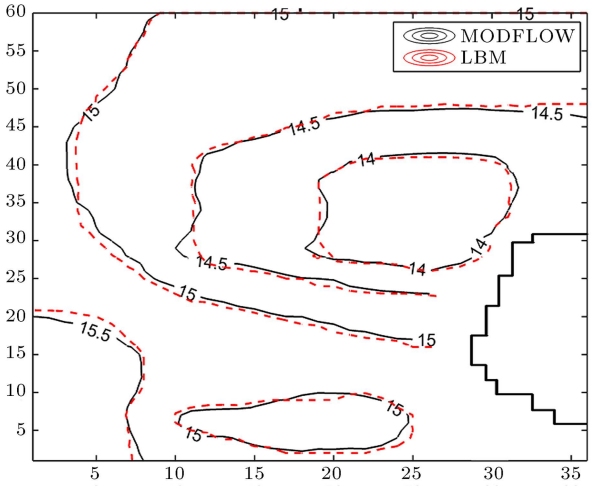

(b)

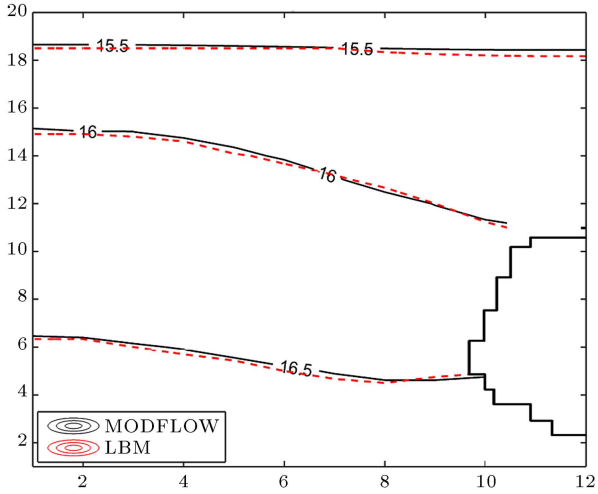

(c)

Figure 7. Head contour obtained from MODFLOW and Lattic Boltzmann Method (LBM): (a) step one, (b) step two, and (c) step three (Problem 2).

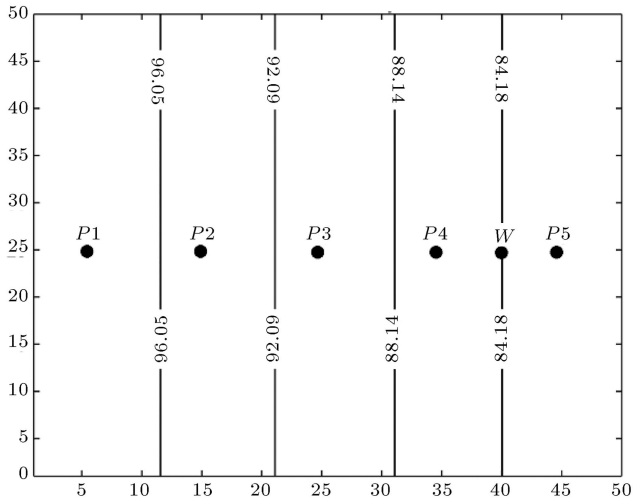

Figure 8. Plan view of aquifer and initial head for step one (Problem 3).

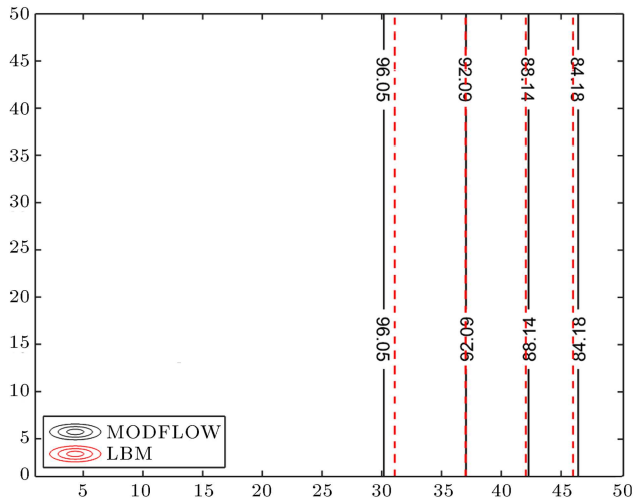

(a)

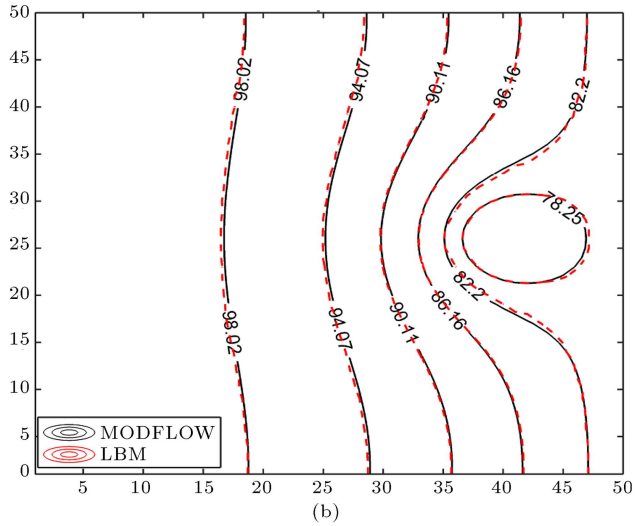

(b)

Figure 9. Head contour obtained from MODFLOW and Lattic Boltzmann Method (LBM): (a) step one, and (b) step two (Problem 3).

distribution function was introduced for this purpose. Three different steady and transient problems were solved with the introduced LBM. Different conditions of boundary conditions and several states of recharge and pumping rate were also considered in the problems. The results indicated that the introduced LBM gives rise to a satisfactory numerical solution for the groundwater flow in unconfined aquifers, wherein the state variable is of second order.

References

1. Zhou, J.G. "Lattice Boltzmann method for advection and anisotropic dispersion equation", *J. Appl. Mech.*, **78**(2), pp. 1–5 (2011).

2. Hekmatzadeh, A.A., Adel, A., Zarei, F., and Haghighi, A.T. "Probabilistic simulation of advection-reaction-dispersion equation using random lattice Boltzmann method", *Int. J. Heat Mass Transf.*, **144**, p. 118647 (2019).

3. Hekmatzadeh, A.A., Keshavarzi, H., Talebbeydokhti, N., and T. Haghighi, A. "Lattice Boltzmann solution of advection-dominated mass transport problem: A comparison", *Sci. Iran.*, **27**(2), pp. 625–638 (2020).

4. Wang, H. "Numerical simulation for solitary wave of Klein-Gordon-Zakharov equation based on the lattice Boltzmann model", *Comput. Math. with Appl.*, **78**(12), pp. 3941–3955 (2019).

5. Zhao, Y., Wu, Y., Chai, Z., and Shi, B. "A block triple-relaxation-time lattice Boltzmann model for nonlinear anisotropic convection-diffusion equations", *Comput. Math. with Appl.*, **79**(9), pp. 2550–2573 (2020).

6. Salinas, Á., Torres, C., and Ayala, O. "A fast and efficient integration of boundary conditions into a unified CUDA Kernel for a shallow water solver lattice Boltzmann method", *Comput. Phys. Commun.*, **249**, p. 107009 (2020).

7. Chen, Y. and Müller, C. "A Dirichlet boundary condition for the thermal lattice Boltzmann method", *Int. J. Multiph. Flow*, **123**, p. 103184 (2020).

8. Aristov, V.V., Ilyin, O.V., and Rogozin, O.A. "Kinetic multiscale scheme based on the discrete-velocity and lattice-Boltzmann methods", *J. Comput. Sci.*, **40**, p. 101064 (2020).

9. Vandekerckhove, C., Van Leemput, P., and Roose, D. "Acceleration of lattice Boltzmann models through state extrapolation: a reaction-diffusion example", *Appl. Numer. Math.*, **58**, pp. 1742–1757 (2008).

10. Yu, X., Regenauer-Lieb, K., and Tian, F.-B. "A hybrid immersed boundary-lattice Boltzmann/finite difference method for coupled dynamics of fluid flow, advection, diffusion and adsorption in fractured and porous media", *Comput. Geosci.*, **128**, pp. 70–78 (2019).

11. Mohamad, A., *Lattice Boltzmann Method*, Springer, **70**, pp. 21–100 (2011).

12. Perumal, D.A. and Dass, A.K. "A review on the development of lattice Boltzmann computation of macro fluid flows and heat transfer", *Alex. Eng. J.*, **54**(4), pp. 955–971 (2015).

13. Li, L., Mei, R., and Klausner, J.F. "Lattice Boltzmann models for the convection-diffusion equation: D2Q5 vs D2Q9", *Int. J. Heat Mass Transf.*, **108**, pp. 41–62 (2017).

14. Xia, Y., Wu, J., and Zhang, Y. "Lattice-Boltzmann simulation of two-dimensional super-diffusion", *Eng. Appl. Comput. Fluid Mech.*, **6**(4), pp. 581–594 (2012).

15. Perko, J. and Patel, R.A. "Single-relaxation-time lattice Boltzmann scheme for advection-diffusion problems with large diffusion-coefficient heterogeneities and high-advection transport", *Phys. Rev. E.*, **89**(5), p. 053309 (2014).

16. Chopard, B., Falcone, J.-L., and Latt, J. "The lattice Boltzmann advection-diffusion model revisited", *The Eur. Phys. J. Spec. Top.*, **171**(1), pp. 245–249 (2009).

17. Guo, X., Shi, B., and Chai, Z. "General propagation lattice Boltzmann model for nonlinear advection-diffusion equations", *Phy. Rev. E.*, **97**(4), p. 043310 (2018).

18. Zhang, M., Zhao, W., and Lin, P. "Lattice Boltzmann method for general convection-diffusion equations: MRT model and boundary schemes", *J. Comput. Phys.*, **389**, pp. 147–163 (2019).

19. Xing, H., Dong, X., Sun, D., and Han, Y. "Anisotropic lattice Boltzmann-phase-field modeling of crystal growth with melt convection induced by solid-liquid density change", *J. Mater. Sci. Technol.*, **57**, pp. 26–32 (2020).

20. Gawas, A.S. and Patil, D.V. "Axisymmetric thermal-lattice Boltzmann method for Rayleigh-Bénard convection with anisotropic thermal diffusion", *J. Comput. Sci.*, **45**, p. 101185 (2020).

21. Cartalade, A., Younsi, A., and Neel, M.C. "Multiple-relaxation-time Lattice Boltzmann scheme for fractional advection-diffusion equation", *Comput. Phys. Commun.*, **234**, pp. 40–54 (2019).

22. Chai, Z. and Shi, B. "Multiple-relaxation-time lattice Boltzmann method for the Navier-Stokes and nonlinear convection-diffusion equations: Modeling, analysis, and elements", *Phys. Rev. E.*, **102**(2), p. 023306 (2020).

23. Yan, Z., Yang, X., Li, S., and Hilpert, M. "Two-relaxation-time lattice Boltzmann method and its application to advective-diffusive-reactive transport", *Adv. Water Resour.*, **109**, pp. 333–342 (2017).

24. Guo, C., Zhao, W., and Lin, P. "On the collision matrix of the lattice Boltzmann method for anisotropic convection-diffusions equations", *Appl. Math. Lett.*, **105**, p. 106304 (2020).

25. Zhang, H. and Misbah, C. "Lattice Boltzmann simulation of advection-diffusion of chemicals and applications to blood flow", *Comput. Fluids.*, **187**, pp. 46–59 (2019).

26. Du, R. and Liu, Z. "A lattice Boltzmann model for the fractional advection-diffusion equation coupled with incompressible Navier-Stokes equation", *Appl. Math. Lett.*, **101**, p. 106074 (2020).

27. Wolf-Gladrow, D. "A lattice Boltzmann equation for diffusion", *J. Stat. Phys.*, **79**(5–6), pp. 1023–1032 (1995).

28. Lin, Y., Yang, C., Choi, C., et al. "Lattice Boltzmann simulation of multicomponent reaction-diffusion and coke formation in a catalyst with hierarchical pore structure for dry reforming of methane", *Chem. Eng. Sci.*, **229**, p. 116105 (2020).

29. Zhou, J.G. "A lattice Boltzmann model for groundwater flows", *Int. J. Mod. Phys. C.*, **18**(06), pp. 973–991 (2007).

30. Zhou, J.G. "A rectangular lattice Boltzmann method for groundwater flows", *Mod. Phys. Lett. B.*, **21**(09), pp. 531–542 (2007).

31. Anwar, S. and Sukop, M.C. "Regional scale transient groundwater flow modeling using lattice Boltzmann methods", *Comput. Math. With Appl.*, **58**(5), pp. 1015–1023 (2009).

32. Budinski, L., Fabian, J., and Stipić, M. "Lattice Boltzmann method for groundwater flow in non-orthogonal structured lattices", *Comput. Math. with Appl.*, **70**, pp. 2601–2615 (2015).

33. Anwar, S. and Sukop, M.C. "Lattice Boltzmann models for flow and transport in saturated karst", *Groundw.*, **47**(3), pp. 401–413 (2009).

34. Abdelaziz, R., Pearson, A.J., and Merkel, B.J. "Lattice Boltzmann modeling for tracer test analysis in a fractured Gneiss aquifer", *Nat. Sci.*, **5**(3), pp. 368–374 (2013).

35. Liu, X., Huang, Y., Wang, C.H., and Zhu, K. "Solving steady and transient radiative transfer problems with strong inhomogeneity via a lattice Boltzmann method", *Int. J. Heat Mass Transf.*, **155**, p. 119714 (2020).

36. Todd, D.K. and Mays, L.W., *Groundwater Hydrology*, John Wiley & Sons (2004).

37. Zhou, J.G., *Lattice Boltzmann Methods for Shallow Water Flows*, Springer, **4** (2004).

38. Girimaji, S. "Lattice Boltzmann method: Fundamentals and engineering applications with computer codes. 2013", *AIAA J.*, **51**(1), pp. 278–279 (2013).

39. El-Ghandour, H.A. and Elsaid, A. "Groundwater management using a new coupled model of flow analytical solution and particle swarm optimization", *Int. J. Water Resour. Environ. Eng.*, **5**(1), pp. 1–11 (2013).

40. Malama, B. "Alternative linearization of water table kinematic condition for unconfined aquifer pumping test modeling and its implications for specific yield estimates", *J. Hydrol.*, **399**(3–4), pp. 141–147 (2011).

41. Moench, A.F. "Combining the Neuman and Boulton models for flow to a well in an unconfined aquifer", *Groundw.*, **33**(3), pp. 378–385 (1995).

42. Moench, A.F. "Flow to a well in a water-table aquifer: an improved Laplace transform solution", *Groundw.*, **34**(4), pp. 593–597 (1996).

43. Moench, A.F. "Flow to a well of finite diameter in a homogeneous, anisotropic water table aquifer", *Water Resour. Res.*, **33**(6), pp. 1397–1407 (1997).

44. Blumenthal, B.J. and Zhan, H. "Rapid computation of directional wellbore drawdown in a confined aquifer via poisson resummation", *Adv. Water Resour.*, **94**, pp. 238–250 (2016).

45. Malama, B., Kuhlman, K.L., and Barrash, W. "Semi-analytical solution for flow in leaky unconfined aquifer-aquitard systems", *J. Hydrol.*, **346**(1–2), pp. 59–68 (2007).

46. Chiang, W. "Processing modflow: an integrated modeling environment for the simulation of groundwater flow, transport and reactive processes, users manual, manuscript", *Simcore Software* (2010).

Biographies

Roghayeh Yousefi received a PhD degree in Civil Engineering from Shiraz University, Iran, in 2019, and an MS degree in Water Engineering, in 2013, from Shahid Chamran University, Iran. Her research interests include numerical modeling of groundwater and pollution transport as well as hydraulic structures.

Nasser Talebbeydokhti is a Professor of Civil and Environmental Engineering at Shiraz University, Iran, since 1984. He is currently a member of the Academy of Science and Editor_in_Chief of the Iranian Journal of Science and Technology, Transaction of Civil Engineering. In recognition of his works and significant contributions, he was the recipient of the 2017 nationwide distinguished professor at Ministry of Higher Education, for demonstrated excellence in the areas of teaching, research, instruction, university service, and public service. He was also the recipient of the Distinguished Hydraulic Professor by the Iran Hydraulic Society.

Seyyed Hosein Afzali is currently an Associate Professor of Civil and Environmental Engineering at Shiraz University, Shiraz, Iran. His research interests include

groundwater, hydraulic structures, river engineering, optimization problems, and fluid mechanics.

Ali Akbar Hekmatzadeh is currently an Associate Professor of Civil and Environmental Engineering at Shiraz University of Technology, Iran, since 2014. He received BSc, MSc, and PhD degrees, all in Civil and Environmental Engineering from Shiraz University, Iran. His areas of research are groundwater modeling and pollution transport, hydraulic structures, water treatment processes, in addition to reliability in engineering problems and hydrology.